

A Comprehensive Theory Based Transport Model

G.M. Staebler 1), J.E. Kinsey 2), and R.E. Waltz 1)

1) General Atomics, P.O. Box 85608, San Diego, California 92186-5608, USA

2) Lehigh University, Bethlehem, Pennsylvania, USA

e-mail contact of main author: gary.staebler@gat.com

Abstract. A new theory based transport model with comprehensive physics (trapping, general toroidal geometry, fully electromagnetic, electron-ion collisions, impurity ions) has been developed. The core of the model is the new trapped-gyro-Landau-fluid (TGLF) equations which provide a fast and accurate approximation to the linear eigenmodes for gyrokinetic drift-wave instabilities (trapped ion and electron modes, ion and electron temperature gradient modes and kinetic ballooning modes). The new TGLF transport model is more accurate, and has an extended range of validity, compared to its predecessor GLF23. The TGLF model unifies trapped and passing particles in a single set of gyro-Landau-fluid equations. A model for the averaging of the Landau resonance by the trapped particles makes the equations work seamlessly over the whole drift-wave wavenumber range from trapped ion modes to electron temperature gradient modes. A fast eigenmode solution method enables unrestricted magnetic geometry. The transport model uses the TGLF eigenmodes to compute quasilinear fluxes of energy and particles. A model for the saturated intensity of the turbulence completes the flux calculation. The intensity model is constructed to fit a large set of nonlinear gyrokinetic turbulence simulations with kinetic electrons. The TGLF model is valid in new physical regimes that GLF23 was not. For example, the low aspect ratio spherical torus which has both a high trapped fraction and strong shaping of magnetic flux surfaces. The TGLF model is also valid close to the magnetic separatrix so the transport physics of the H-mode pedestal region can be explored.

1. Introduction

Even the largest computers available today still cannot simulate the turbulent transport in a full radius tokamak plasma with kinetic electrons and ions to predict temperature and density profiles consistent with the power and particle sources. Hence, there is a need for reduced models of the turbulent transport. The term “theory-based modeling” is used here to mean models that are designed to fit more exact theory rather than empirically fit to data. The multi-mode model [1,2] established a methodology for quasilinear transport models later used in GLF23 [3]. The GLF23 model uses a set of gyro-Landau fluid (GLF) equations that included kinetic effects like gyro-averaging and Landau damping. The linear modes are found numerically and a formula for the intensity of the saturated turbulence is used to complete the quasilinear calculation of energy and particle fluxes. The formula for the intensity was designed to fit nonlinear GLF turbulence simulations [4-6] since these were state-of-the-art at the time (1996).

The main strength of a theory-based model is that comparing the model to experiment is a test of the theory it represents. GLF23 and the multi-mode models have had great success in L-mode and H-mode core plasmas where the low-k physics is dominant [7]. The high-k electron temperature gradient mode (ETG) was demonstrated by GLF23 to give about the right level of electron thermal transport in regions where the ExB velocity shear had quenched the low-k ion temperature gradient (ITG) and trapped electron mode (TEM) [3]. In fact when GLF23 was built, it was only a conjecture that TEM mode turbulence could be suppressed by ExB velocity shear, although it had been shown that it could be linearly stabilized [8]. The quenching of TEM modes has recently been demonstrated in gyrokinetic turbulence simulations [9].

In addition to these areas where the theory agrees with experiment, deficiencies of the theory have been found. The ETG modes in GLF23 do not produce any particle flux or ion thermal or momentum transport because the ions are assumed to be adiabatic for high- k . However, in experiments with strong ExB velocity shear and measured ion thermal transport at neoclassical levels, the particle and ion toroidal momentum transport does not reduce to the predicted neoclassical levels. One possible explanation for this phenomenon is that the cascade of high- k ETG modes to low- k could produce the required transport. Nonlinear gyrokinetic simulations of high- k ETG modes coupled to low- k ITG/TEM modes are just now becoming possible. The new trapped gyro-Landau fluid (TGLF) model unifies trapped and passing electrons into a single set of equations that are not restricted by wavenumber or frequency regimes. This makes TGLF capable of modeling the new nonlinear gyrokinetic turbulence simulations of coupled ETG and ITG modes.

The GLF23 model was kept small and fast due to the speed of computers in 1996. With faster computers a more accurate system of moment equations can be used. Sec. 2 will introduce the new features of TGLF compared to its predecessor GLF23 and give some examples of linear stability calculations for an experimental tokamak discharge. Section 3 presents the model for the intensity derived from fitting to nonlinear gyrokinetic turbulence simulations. The concluding Sec. 4 discusses the applications of the TGLF model.

2. TGLF Moment Equations

A full presentation of the derivation and closure of the TGLF equations is given in Ref. 10. The complete system has 12 moments for circulating particles and 3 for trapped particles, for each species. The ballooning representation wave function is typically expanded in four Hermite basis functions so the eigenvalues of a 120x120 complex matrix needs to be solved for each toroidal mode number for a pure plasma. The use of four basis functions instead of just one is crucial for shaped geometry. By comparison GLF23 has a low- k and a high- k system of equations. For low- k there are four equations for circulating ions (no trapped ions), two for circulating electrons, and two for trapped electrons. For high- k there is a four moment system of equations for circulating electrons with adiabatic ions. GLF23 uses a parameterized trial wave function so an 8x8 complex matrix eigenvalue problem must be solved for each low- k mode number and a 4x4 system for each high- k mode number. The “gyro” in gyro-Landau fluid (GLF) refers to the inclusion of finite Larmor radius (FLR) effects due to gyro-averaging. Without trapped particles the TGLF equations are very close to the GLF model of Beer and Hammett [5]. Their method of closing the GLF equations was used to close the TGLF equations. The inclusion of trapped particles makes the TGLF equations more complicated. The closure coefficients need to be functions of the trapped fraction and a more exact treatment of the FLR terms was required in order for the equations to be valid for both low and high- k . An FLR correction to the closure coefficients was also needed. The untrapped moments of the distribution function are split into two parts, one moment is over all of velocity space and the other moment is over the trapped region which is subtracted from the total velocity moment to get the untrapped moments. The impact of the trapped region on the circulating particles is much better represented in TGLF than in previous GLF equations. The cost is twice as many moment equations for the circulating particles. The three moments used for the trapped particles gives a trapped particle density response functions which is as accurate as the bounce averaged model of Ref. 6. It is much more accurate than the 2-moment trapped electron model of GLF23. All previous GLF models for including trapped particles relied on an ordering of the frequency to the bounce frequency of the trapped particle [3,4,6]. An important new feature of the TGLF equations is a model for the boundary between

trapped particles that can average the Landau resonance and those that cannot. This model is built into the definition of the effective trapped fraction that varies with the parallel wavenumber rather than the mode frequency. This allows the same set of equations to be used for all frequencies and poloidal wavenumbers.

This is illustrated in Fig. 1 where the TGLF calculation of the spectrum of linear growth rates (solid) is compared to the spectrum computed with the initial value gyrokinetic code GKS [11] (dashed). Data from an actual experimental discharge at the flux surface $r/a=0.7$ was used. The discharge is 84736 from the DIII-D tokamak as described in Ref. 12. Both calculations have dynamic electrons, deuterium and carbon ions, shaped Miller geometry [13], electron-ion collisions and electromagnetic finite beta physics included. Much of this physics has been added to TGLF since the publication of Ref. 10. The system of units used is $c_s = \sqrt{T_e/m_i}$, $\rho_s = c_s/\Omega_s$, $\Omega_s = eB/m_i c$. The normalized growth rate, frequency and poloidal wavenumber are $\hat{\gamma} = \gamma(a/c_s)$, $\hat{\omega} = \omega(a/c_s)$, $k_y = \rho_s k_\theta$. As is typical for TGLF, the agreement with GKS for the growth rate in Fig. 1 is better than for the frequency. This is because the frequency depends more sensitively on the shape of the wave function. These TGLF calculations are done with only four Hermite basis functions to resolve the wave function. Adding more basis functions improves the frequency but typically has a smaller impact on the growth rate. Since it is usually more important to know the value of the growth rate than the frequency, and the computation time scales like the square of the number of basis functions, only four basis functions are typically used. The GLF23 model assumes that there is a stable region between the low- k ($k_y < 1$) ITG/TEM modes and the high- k ($k_y > 1$) ETG modes. This assumed spectral instability gap is realized for many discharges deeper in the core, but in the outer 30% of the plasma cross section the linear growth rate spectrum is typically continuous from low to high k_y , as is the case in Fig. 1. GLF23 is not designed to handle the intermediate region $k_y \sim 1$.

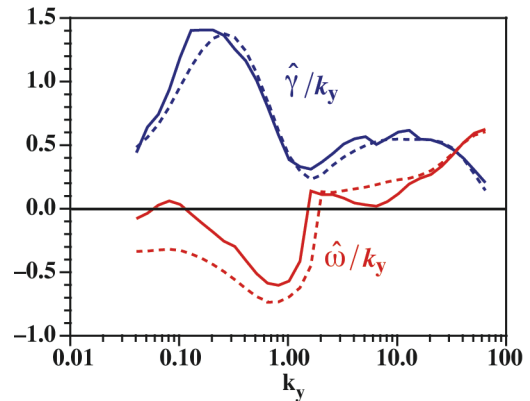


FIG. 1. Comparison of TGLF (solid) and GKS (dashed) growth rate and frequency spectrum for DIII-D discharge 84736 at $r/a=0.7$.

In Fig. 2 the quasilinear weights from TGLF and GKS are compared. The agreement is surprisingly good considering the low resolution used for the TGLF wave functions. The main difference is near the point where the electron mode ($\hat{\omega} > 0$) becomes dominant ($k_y \sim 2$) which is at a slightly lower k_y for TGLF than for GKS in this case. The electrostatic part of the quasilinear weights are the fluxes for a single mode divided by the mode intensity. The ion energy flux, electron energy flux, and particle flux are respectively

$$Q_{i,ql} = \frac{3}{2} \frac{n_i T_i}{n_e T_e} \text{Re} \left[ik_y \tilde{\Phi}^* \tilde{p}_i \right] / |\tilde{\Phi}|^2 \quad Q_{e,ql} = \frac{3}{2} \text{Re} \left[ik_y \tilde{\Phi}^* \tilde{p}_e \right] / |\tilde{\Phi}|^2 \quad \Gamma_{ql} = \text{Re} \left[ik_y \tilde{\Phi}^* \tilde{n}_e \right] / |\tilde{\Phi}|^2 ,$$

where $(\tilde{n}_e, \tilde{p}_e, \tilde{p}_i)$ are the electron density, electron total pressure and ion total pressure moments of the perturbed distribution function normalized to their equilibrium values. The normalized electrostatic potential fluctuation is $\tilde{\Phi} = e\tilde{\phi}/T_e$. Notice that even though the ion energy flux weight in Fig. 2 drops near zero above $k_y=2$ where the most unstable mode

becomes an electron mode (Fig. 1), the particle flux retains a non-zero (negative in this case) weight well above this point where the ions are being damped by finite Larmor radius effects.

The linear stability of the TGLF equations has been extensively benchmarked with the GKS code. A large set (1799) of scans of plasma parameters (a/L_{ne} , a/L_{ni} , a/L_{Te} , a/L_{Ti} , T_i/T_e , q , \hat{s} , α , k_y , r/a , R/a) in shifted circle (s -alpha) geometry were used. The fractional deviation (standard deviation divided by the root mean squared average for GKS) of the growth rate for a subset of these scans is shown in Fig. 3. These are all scans about a reference point with parameters relevant to an H-mode pedestal (PED) = ($a/L_{ne}=a/L_{ni}=3$, $a/L_{Ti}=a/L_{Te}=10$, $T_i/T_e=1$, $q=4$, $\hat{s}=3$, $\alpha=5$, $k_y=0.3$, $r/a=0.5$, $R/a=3$). Each bar of the histogram (Fig. 3) has eighty cases with the magnetic shear and safety factor varied over the ranges ($1 \leq \hat{s} \leq 7$, $3 \leq q \leq 7$). The normalized pressure gradient α was increased from 0 to 12 as labeled. Also shown are the statistics for the GLF23 model. The most recent version of GLF23 [14] was used and even though the trial wavefunction in this version was re-tuned to include a dependence on $\hat{s} - \alpha$ it is clear that the GLF23 model becomes inaccurate when $|\hat{s} - \alpha| > 1$. The TGLF model maintains its good accuracy for all of the scans. The average fractional deviation of all of the 1799 cases was 11.4% for the TGLF growth rates.

The inclusion of shaped Miller geometry, electromagnetic fluctuations, electron-ion collisions and impurity ions did not require changing the closure coefficients for TGLF. In Fig. 4 is shown an example of the impact of this physics on the linear growth rates for DIII-D discharge 84736. The normalized growth rate profile for $k_y=0.3$ for both GKS (dashed) and TGLF (solid) are compared for three different physics settings. The lowest pair of curves (A) are with all the physics turned on. The middle pair of curves (B) are with collisions and electromagnetic terms omitted. The highest pair of curves (C) are with shifted circle geometry and impurities treated as dilution (no response) in addition to being collisionless and electrostatic like B. The difference between (C and B) is mostly due to the change to shifted circle geometry with a small increase in growth rate for dilution compared to full impurity dynamics (fully stripped carbon assumed) as the impurity concentration increases towards the edge. The

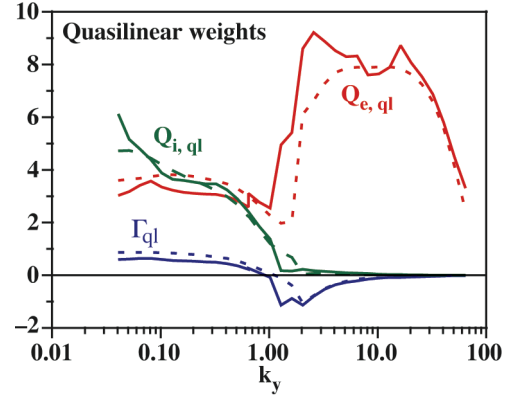


FIG. 2. Comparison of the quasilinear weights from TGLF (solid) and GKS (dashed) corresponding to the modes in Fig. 1.

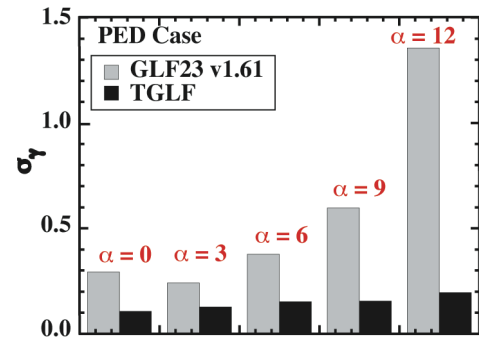


FIG. 3. Fractional deviation of the growth rate (σ_γ) from GKS for five scans for GLF23 (grey) and TGLF (black).

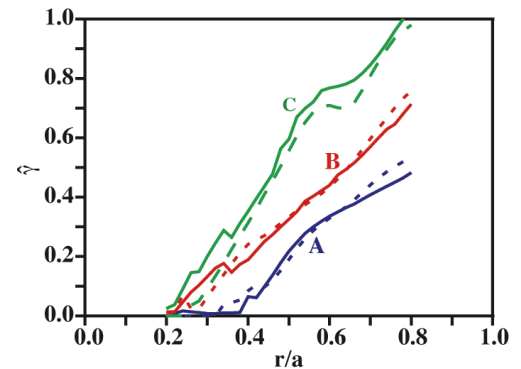


FIG. 4. TGLF (solid) and GKS (dashed) growth rates for discharge 84736 and $k_y=0.3$ for 3 sets of physics setting A, B, C.

difference between (C and B) is mostly due to the change to shifted circle geometry with a small increase in growth rate for dilution compared to full impurity dynamics (fully stripped carbon assumed) as the impurity concentration increases towards the edge. The

difference between B and A is mostly due to electron-ion collisions although the electromagnetic effects have a stabilizing impact for $r/a < 0.5$. At the analysis time of 1.3 s, 84736 had negative central shear with $q_{\min} = 1.8$ at $r/a = 0.4$ and $q = 2.9$ at $r/a = 0$. The elongation was 2.0 and the average triangularity was 0.88 at the last closed flux surface. The growth rate analysis is not extended out to the edge in Fig. 4 because a much higher resolution magnetic equilibrium is needed in order to get accurate plasma profiles and geometry in the near separatrix region. The tools to accomplish this task are not yet completely installed for the linear stability code.

3. TGLF Transport Model

The fluxes due to individual linear eigenmodes can be calculated using quasilinear theory. The saturated intensity of the potential fluctuations is not computable from first principles but must be obtained from a formula fit to nonlinear turbulence simulations. The TGLF transport model uses a saturation rule that is local in space and local in k_y . That is, the flux due to each k_y -eigenmode is computed and there is no model for coupling between modes (non-local in k_y) or from one flux surface to another (non-local in space). A local model for the saturated potential fluctuation intensity should be constructed from local quantities like the growth rate of the linear instability or plasma properties at the flux surface.

A database of nonlinear turbulence simulations using the GYRO [15] gyrokinetic code has been assembled [16]. From this database of over 300 runs, 86 cases that were grouped in scans of individual plasma parameters about three base points were chosen. Only shifted circle geometry cases are included. The contribution to the fluxes of energy and particles from each toroidal mode number ($ky = \rho_s(nq/r)$, n is the toroidal mode number) in the GYRO simulation is used to find the best fit for a local saturation rule. All of the simulations had 16 toroidal modes including $n = 0$, but the fixed spacing between modes was adjusted to insure that the peak in the flux spectrum was resolved. Most of the cases had a spacing between modes of $\Delta_{ky} = 0.05$. The total flux is the sum over k_y of the individual mode contributions. Only the most unstable mode at each k_y is used but subdominant mode contributions could be added to future models.

The model for the normalized fluxes at each k_y is

$$\hat{Q}_i = c_{Q_i} \bar{\Phi}^2 Q_{i,ql} \quad , \quad \hat{Q}_e = c_{Q_e} \bar{\Phi}^2 Q_{e,ql} \quad , \quad \hat{\Gamma} = c_{\Gamma} \bar{\Phi}^2 \Gamma_{ql} \quad ,$$

These fluxes are normalized to the gyro-reduced flux, $n_e T_e c_s \rho_*^2$ for energy and $n_e c_s \rho_*^2$ for particle flux, with $\rho_* = \rho_s/a$. The three coefficients ($c_{Q_i} = 30.0$, $c_{Q_e} = 32.4$, $c_{\Gamma} = 36.6$) are determined by the constraint that the offset between the TGLF and GYRO fluxes summed over the whole database be zero. All three coefficients would be the same if the quasilinear theory were in exact agreement with GYRO. The differences correct the systematic trends for the quasilinear weights to be either high or low. The intensity for the gyro-reduced norm is $\bar{\Phi}^2 = \tilde{\Phi}^2 / \rho_*^2$. The formula for the intensity of the most unstable mode at each k_y is given by

$$\bar{\Phi}^2 = \Delta_{ky} \frac{\hat{\omega}_{d0}^2}{k_y^4} \Lambda \quad , \quad \Lambda = \frac{\bar{\gamma}^{\beta_\gamma} \left[\alpha_{d0} + (\alpha_d \bar{\omega}_d)^{\beta_d} \right]}{\left[1 + (\alpha_\gamma \bar{\gamma})^{\beta_\gamma} \right] \left[1 + (\alpha_d \bar{\omega}_d)^{\beta_d} \right] k_y^{\beta_k}} \quad , \quad \hat{\omega}_{d0} = k_y (a/R) \quad ,$$

$$\bar{\omega}_d = \left| \langle \hat{\omega}_d \rangle \right| / \hat{\omega}_{d0} \quad , \quad \bar{\gamma} = \text{Max} \left[\left(\hat{\gamma} - \alpha_{ZF} / \hat{\gamma}_{ZF} - \alpha_E \hat{\gamma}_{ExB} \right) / \hat{\omega}_{d0}, 0 \right] \quad ,$$

$$\hat{\gamma}_{ZF} = \hat{\omega}_{d0} \left(\hat{\gamma} / \hat{\omega}_{d0} \right)^{\beta_{zg}} / \left(k_y^{\beta_{zk}} q^{\beta_{zq}} \right) \quad .$$

Note the inclusion of the ExB velocity shear $\hat{\gamma}_{ExB}$ in the net growth rate $\bar{\gamma}$. The local growth rate normalization is taken to be the curvature drift at the outboard midplane $\hat{\omega}_{d0}$ so that $\bar{\gamma}$ is independent of the global length scale “a”. The model for the effective ExB velocity shear rate due to zonal flows $\hat{\gamma}_{ZF}$ is taken to depend only on the growth rate of the mode at k_y , like the formula for the intensity. Both of these are actually sums over all of the modes and such non-local in k -space intensity rules will be investigated in the future. The dependence on the absolute value of the curvature drift averaged with the Gaussian width of the wavefunction $\bar{\omega}_d$ is needed in order to obtain good fits for negative local magnetic shear. The fit coefficients are found by minimizing an error function that includes both deviations of the spectrally resolved fluxes and deviations of the total fluxes in a weighted sum. The result is: $\alpha_\gamma=0.893$, $\beta_\gamma=1.98$, $\beta_k=0.933$, $\alpha_d=2.55$, $\beta_d=1.94$, $\alpha_{d0}=0.072$. $\alpha_{ZF}=0.369$, $\beta_{z\gamma}=0.906$, $\beta_{zk}=0.420$, $\beta_{zq}=0.317$, $\alpha_E=0.17$. From a simple dimensional argument, balancing the ExB nonlinearity rate against the growth rate, one would expect $\bar{\Phi}^2 \propto \hat{\gamma}^2 / k_y^4$. The numerical best fit is close to this for the growth rate with $\beta_\gamma \sim 2$ but not for k_y . For strong growth rates, the model gives an intensity that becomes asymptotically independent of the growth rate. This is required in order to model the large gradient GYRO simulations. The model has not yet been tested for simulations with high-k ETG modes and it is expected that some changes will be necessary to extend into this range.

Normalized total fluxes computed using the TGLF model are plotted against the GYRO total fluxes in Fig. 5. The fractional deviation for the whole database of 86 cases is $\sigma_{Q_i}=17\%$, $\sigma_{Q_e}=15\%$, $\sigma_\Gamma=28\%$. The fractional deviation for the particle flux is largest partly because the root mean squared flux is smaller. A negative particle flux means the flow is against the density gradient.

The TGLF fluxes are a much better fit to GYRO than is GLF23. Shown in Fig. 6 is a comparison of the fluxes from TGLF (solid) and GLF23 (dot-dashed) to the GYRO nonlinear simulation result (dashed) for a temperature gradient scan about the standard point (STD) with parameters $(a/L_{ne} = a/L_{ni} = 1, a/L_{Te} = a/L_{Ti} = 3, T_i/T_e=1, q=2, \hat{s}=1, \alpha=0, r/a=0.5, R/a=3.0)$. Both the threshold and slope of the GYRO fluxes are a much better fit by TGLF. The electron energy flux is systematically high for GLF23 in Fig. 6 and for the whole database of 86 GYRO cases. GLF23 was designed to fit this same temperature gradient scan but with adiabatic electrons [7].

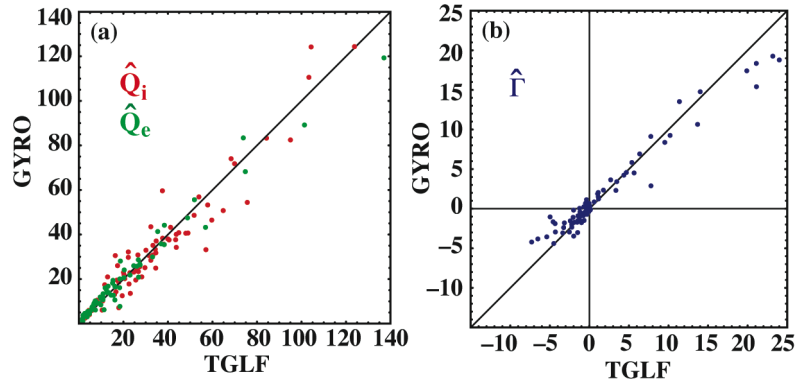


FIG. 5. Comparison of ion (red) and electron (green) energy flux (a) and particle flux (b) from GYRO nonlinear simulation to the TGLF model.

A remarkable result is that the GYRO transport flux spectrum is very well fit by this quasilinear model. In Fig. 7(a-c) are shown the spectrally resolved fluxes for the standard case (STD). The fit is best for the ion energy flux [Fig. 7(b)] and the most unstable mode is an ion mode for the whole spectrum in this case. There are two nonlinear features of the model. The first is the zonal flow shear rate. In Fig. 7(d) is shown the impact of turning off the zonal flow shear $\alpha_{ZF}=0$. The zonal flow shear is critical in suppressing the low- k modes which would otherwise contribute greatly to the fluxes. The zonal flow shear model also provides a nonlinear upshift in the critical gradient similar to the Dimit shift [18] seen in gyrokinetic turbulence simulations.

The other nonlinear effect is that the intensity of each individual k_y mode is proportional to the spacing between modes Δ_{k_y} . This factor is needed in order for the sum over the spectrum to be approximately independent of the spacing or number of modes. Physically this must be due to the nonlinear coupling between toroidal mode numbers spreading the turbulence over the spectrum. The flux weights must not be greatly changed by nonlinear interactions since the quasilinear model works so well.

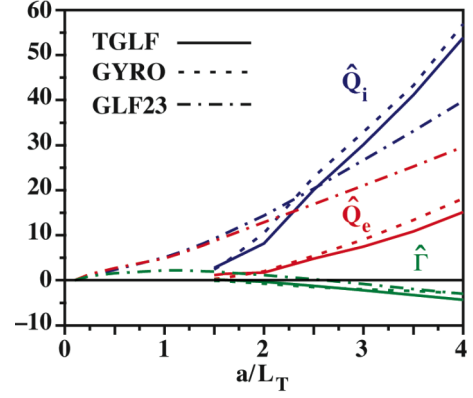


FIG. 6. Comparison of normalized fluxes for TGLF (solid) GYRO (dashed) and GLF23 (dot-dashed) for a scan in $a/L_{Ti} = a/L_{Te}$ about the STD point.

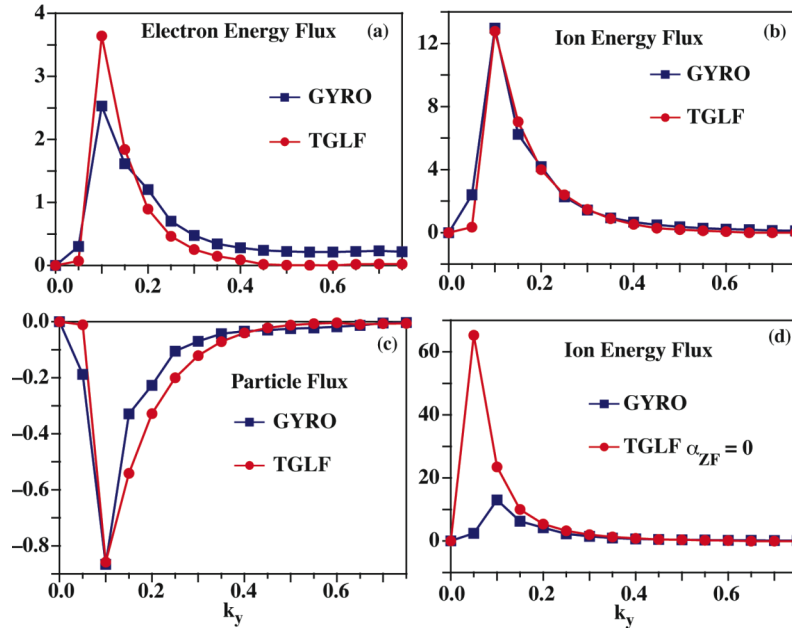


FIG. 7. Comparison of the nonlinear GYRO spectrum and TGLF transport model for the STD case. Electron energy flux (a), ion energy flux (b), particle flux (c), and ion energy flux with the zonal flow shear turned off (d).

4. Summary and Applications

The trapped gyro-Landau fluid model TGLF has a number of innovations that allow the unification of trapped and passing particles into a system of moment equations. The equations have now been extended to include shaped Miller geometry, electron-ion collisions, fully electromagnetic fluctuations and dynamic impurity ions. The linear eigenmode solver for

TGLF is available as a fast alternative to GKS for linear drift-wave stability analysis of experimental discharges. TGLF can also calculate the eigenvalues for subdominant instabilities that GKS cannot access. Illustrations of the use of TGLF to compute the full k_y spectrum of instabilities at one radius and the radial profile at a single k_y for an experimental discharge were given. It is planned to make the TGLF linear stability code available for between discharge control room analysis. This should be useful as a guide for experiments seeking to modify the drift-wave instabilities. Even the density fluctuation level can be estimated using the model for the saturated intensity. Using a large database of nonlinear GYRO runs (86) a model for the fluctuation level of the turbulence has been constructed to fit the spectrally resolved fluxes of energy and particles. Even the detailed shape of the nonlinear spectra are well fit by the quasilinear TGLF transport model. The new transport model will be tested with experimental data in the near future. It should be possible to use the TGLF transport model in the near separatrix region even in H-mode. TGLF is the first transport model that is valid for low aspect ratio spherical tori. A model for the saturation of high-k ETG modes will be developed based on recent gyrokinetic simulations with kinetic ions. The ExB velocity shear has been included using the quench rule as in GLF23. It is planned to investigate methods to include both ExB and parallel velocity shear in the linear eigenmodes so that the quasilinear weights and viscous stress tensor can be computed with both velocity shears. Models for the saturated fluctuation intensity that are nonlocal in k_y or space will be investigated.

This work was supported by the U.S. Department of Energy under DE-FG03-95ER54309 and DE-FG02-92ER54141.

References

- [1] KINSEY, J.E., and BATEMAN, G., *Phys. Plasmas* **3** (1996) 3344.
- [2] BATEMAN, G., *et al.*, *Phys. Plasmas* **5** (1998) 1793.
- [3] WALTZ, R.E., *et al.*, *Phys. Plasmas* **4** (1997) 2482.
- [4] WALTZ, R.E., *et al.*, G.W., *Phys. Plasmas* **2** (1995) 2408; *ibid* **1** (1994) 2229.
- [5] BEER, M.A., and HAMMETT, G.W., *Phys. Plasmas* **3** (1996) 4046.
- [6] BEER, M.A., and HAMMETT, G.W., *Phys. Plasmas* **3** (1996) 4018.
- [7] KINSEY, J.E., WALTZ, R.E., DeBOO, J.C., *Phys. Plasmas* **6** (1999) 1865.
- [8] DOMINGUEZ, R.R., and STAEBLER, G.M., *Phys. Fluids* **B5** (1993) 3876.
- [9] KINSEY, J.E., WALTZ, R.E., CANDY, J., *Phys. Plasmas* **12** (2005) 062302.
- [10] STAEBLER, G.M., KINSEY, J.E., WALTZ, R.E., *Phys. Plasmas* **12** (2005) 102508.
- [11] KOTSCHENREUTHER, M., *et al.*, *Compt. Phys. Commun.* **88** (1995) 128.
- [12] LAO, L.L., *et al.*, *Phys. Plasmas* **3** (1996) 1951.
- [13] MILLER, R.L., *et al.*, *Phys. Plasmas* **5** (1998) 973.
- [14] KINSEY, J.E., STAEBLER, G.M., and WALTZ, R.E., *Phys. Plasmas* **12** (2005) 052503.
- [15] CANDY, J., and WALTZ, R.E., *J. Comput. Phys.* **186** (2003) 545.
- [16] The GYRO database can be found at fusion.gat.com/comp/parallel
- [17] DIMITS, A.M., *et al.*, *Nucl. Fusion* **40** (2000) 661.